

Phase-field approach to heterogeneous nucleation

Mario Castro

*Grupo Interdisciplinar de Sistemas Complejos (GISC) &
Escuela Técnica Superior de Ingeniería (ICAI),
Universidad Pontificia Comillas, E-28008 Madrid, Spain*

We consider the problem of heterogeneous nucleation and growth. The system is described by a phase field model in which the temperature is included through thermal noise. We show that this phase field approach is suitable to describe homogeneous as well as heterogeneous nucleation starting from several general hypotheses. Thus we can investigate the influence of grain boundaries, localized impurities, or any general kind of imperfections in a systematic way. We also put forward the applicability of our model to study other physical situations such as island formation, amorphous crystallization, or recrystallization.

I. INTRODUCTION

Processes driven by nucleation and growth have attracted much attention during past decades, from a fundamental point of view [1] and for tailoring some technological applications. Some of them are: the recrystallization of deformed metals [2], controlling the nucleation and growth of islands on terraces in order to get large scale arrays of nanostructures [3], or the manufacturing of thin-film transistors which are the basic devices for some applications as solar cells [4], random access static memories [5], or active matrix-addressed flat-panel displays [6].

In all the above-mentioned processes, a metastable phase decays into a stable one via a fluctuation which produces a critical cluster of atoms (for instance, a critical island in the case of terrace growth, or a critical atom cluster in the case of crystallization). This transition is called nucleation. At a certain fixed temperature, clusters with sizes greater than a critical one become stable nuclei; otherwise they shrink and eventually vanish. Such a critical size arises from the competition between the surface tension and the chemical potential difference between phases, yielding an energy barrier that has to be overcome to build up a critical nucleus. For the examples presented above, the system can be considered, under certain conditions, two dimensional so it is straightforward to write the free energy of circular grain of radius r :

$$\Delta F(r) = 2\pi r\sigma - \pi r^2 \Delta\mu/\Omega, \quad (1)$$

where, σ , $\Delta\mu$, and Ω are the surface tension, the chemical potential difference between phases, and the mean volume occupied by an atom, respectively.

Notwithstanding, in some practical situations this transformation is not perfectly homogeneous due to, for instance, the presence of physical boundaries, such as terrace steps, the interplay between different kinds of particles, or the appearance of impurities [7], or even to some preexisting order embedded in the initial phase formed

during its manufacturing [8]. The lack of uniformity not only catalyzes the transformation but affects the final size distribution of grains [9,10].

Much work has been devoted to the study of homogeneous nucleation in different contexts [1,11–13], and to the so-called site saturation in which nucleation takes place just at the beginning of the transformation [14], but only a few studies were devoted to the intermediate situations in which nucleation is heterogeneous, both in space and in time. The spatial extent of heterogeneity can be measured using the fraction of transformed material (or more generically, the volume fraction of the newly transformed phase) onto the stable phase which often obeys the Kolmogorov-Johnson-Mehl-Avrami (KJMA) equation [15]:

$$X(t) = 1 - \exp\{-[(t - \tau_i)/\tau_c]^m\}, \quad (2)$$

where τ_i is the incubation time, τ_c is the characteristic transformation time, and m is an exponent which characterizes the degree of heterogeneity of the system and its dimensionality [9,10]. For instance, for a two-dimensional system in the two limiting cases, homogeneous nucleation and site saturation, m takes the values 3 and 2, respectively.

There have been some approaches to the problem of heterogeneous nucleation in the past. For instance, Karpov *et al.* [16] generalized the homogeneous case by adding random contributions to the surface tension and the chemical potential, which affects the nucleation rate. A similar *static* approach was followed by Liu [17], who calculated the variation suffered by the surface tension and the chemical potential due to the presence of a circular impurity. Other authors such as Enomoto [18] or Weinberg [19] considered a phenomenological time-dependent nucleation rate to analyze heterogeneous nucleation. More recently, Castro and co-workers [9,10] have introduced a lattice model to determine both time-dependent and spatial effects of heterogeneities.

The main aim of this paper is analyze, both analytically and numerically, the origin and effect of impurities or defects on grain nucleation and subsequent growth.

The rest of the paper is organized as follows. In Sec. II we introduce a phase field model obtained from a functional free energy and report some results for homogeneous nucleation. In Sec. III, we include impurities through the boundary conditions of the main equation and calculate the effect of those impurities in nucleation rate and KJMA exponent. In Sec. IV, we consider a more general case in which the disorder can be due to mechanisms which are different with the ones presented in Sec. III. These mechanisms are introduced as quenched noise. Finally, we end the paper by summarizing the main results in Sec. V, focusing on the applicability of the equations to different physical processes, and discussing further generalizations of the model.

II. EVOLUTION EQUATION

Phase-field models have been widely studied in the last few years, as an efficient computational tool to simulate some moving boundary problems which, in the so-called sharp interface limit (or sometimes thin interface limit, see below), are physically equivalent [14,20–26]. Among them, Jou and Lusk [14] studied homogeneous nucleation and site saturation using a one-field phase field model. The main objection of their approach is the fact that the critical clusters are created *ad hoc* so, on the one hand, the model explains the KJMA equation just by construction and, on the other hand, it cannot explain the existence of an incubation time observed in the experiments. A similar approach was used by Roy *et al.* [12] to study nucleation in a phase field model with nonlocal interactions. Recently, more complex phase field models have been proposed for similar systems: The so-called multiphase-field models [27,28], in which every cluster appearing embedded in the metastable phase is described by its own field and, on the other hand, those models in which the phase field is coupled with another field representing the orientation of crystalline planes [29,30]. The main problem concerning the multiphase-field models is that the free energy depends explicitly on the grain orientation (or phase). This is solved by the second ones but, besides this, what depends on the grain orientation is the grain-boundary velocity. Although this second kind of approach seems to be very promising, in both cases the symmetry under rotations of the grain crystalline planes is broken.

In this paper we are interested only in the overall dynamics of the nucleation process, thus, we simply generalize the model presented in Ref. [14], supplementing it with thermal noise to make explicit the temperature dependence of the system. To make clearer this generalization, we advance that the noise term is the driving force for nucleation, so it is not needed to create artificially critical clusters every integration time step as in Ref. [14].

Let us introduce the main ingredients of the model. We

define an order parameter ϕ , which takes the value -1 in the metastable phase and $+1$ in the stable phase. The grain boundary (which separates both phases) is located at $\phi = 0$ [31]. We also define a free-energy functional which takes into account the grain-boundary energy and the chemical potential difference between phases. Generically, we can define

$$\mathcal{F}[\phi(\mathbf{r}, t)] = \int dx dz \left(\frac{W^2}{2} |\nabla\phi|^2 + f(\phi) - \lambda g(\phi) \right), \quad (3)$$

where $f(\phi)$ and $g(\phi)$ are generic functions of the order parameter: $f(\phi)$ is an even function of ϕ with local minima at ± 1 and $g(\phi)$ breaks the symmetry between phases. As we will see below, W is a typical length scale related to the surface tension, and λ is a dimensionless parameter proportional to the chemical potential difference between phases. We will assume that the system relaxes towards equilibrium according to the following evolution equations [32]:

$$\begin{aligned} \tau \partial_t \phi &= -\frac{\delta \mathcal{F}}{\delta \phi} + \theta \Rightarrow \\ \tau \partial_t \phi &= W^2 \nabla^2 \phi - f_\phi(\phi) + \lambda g_\phi + \theta, \end{aligned} \quad (4)$$

where τ is the typical time scale at which the atoms from a phase incorporate to the other; f_ϕ and g_ϕ denote the partial derivatives of f and g with respect to ϕ . Finally, $\theta(\mathbf{r}, t)$ is a Gaussian white noise which stands for the thermal fluctuations of the system, with zero mean and correlations given by the fluctuation-dissipation theorem [32]:

$$\langle \theta(\mathbf{r}, t) \theta(\mathbf{r}', t') \rangle = 2\tau k_B T \delta(\mathbf{r} - \mathbf{r}') \delta(t - t'), \quad (5)$$

T being the temperature at which the transformation takes place.

To be more specific, we choose

$$f(\phi) = -\phi^2/2 + \phi^4/4, \quad (6)$$

The main advantage of this choice is that Eq. (4) admits a simple stationary solution given by:

$$\phi_0(z) = -\tanh\left(\frac{z}{\sqrt{2}W}\right), \quad (7)$$

which represents a front of characteristic width W placed at $z = 0$. In the same way, we choose [33]:

$$g(\phi) = \phi - \frac{\phi^3}{3}. \quad (8)$$

The main reason to use Eq. (8) instead of the traditional one, $g(\phi) = \phi$, is that, in the first case, \mathcal{F} has local minima at ± 1 independently of the value of λ , otherwise, those minima would be λ dependent.

Using Eq. (7) we can make some considerations about the stability of a given fluctuation. To compare with the classical nucleation theory [34], let us consider the free energy difference between a system which is initially at the

metastable phase, and a circular grain of radius R given approximately by $\phi_0(r - R)$. Thus it can be straightforwardly shown that, in the thin interface limit [22]:

$$\Delta\mathcal{F} \equiv \mathcal{F}[\phi = \phi_0] - \mathcal{F}[\phi = -1] \simeq 2\pi R\sigma_l - \pi R^2\Delta\mu/\Omega, \quad (9)$$

where $\sigma_l = 2\sqrt{2}W/3$ is the surface tension, and $\Delta\mu/\Omega = \lambda\delta g$, with $\delta g = g(+1) - g(-1)$. This equation shows the competition between the gain arising from the reduction of the grain perimeter, and that related to the increasing of its size. As we mentioned above, the critical radius arises from this competition. Thus if we take into account that $\exp[-\Delta\mathcal{F}(R)/k_B T]$ can be interpreted as the barrier that has to be overcome to create a nucleus of radius R , then the critical radius is the one which minimizes that barrier, the one which maximizes $\Delta\mathcal{F}$. Hence

$$R^* = \frac{2\sqrt{2}W}{3\lambda\delta g}, \quad (10)$$

and its corresponding critical free energy is given by

$$\Delta\mathcal{F}^* = \frac{8\pi W^2}{9\lambda\delta g}. \quad (11)$$

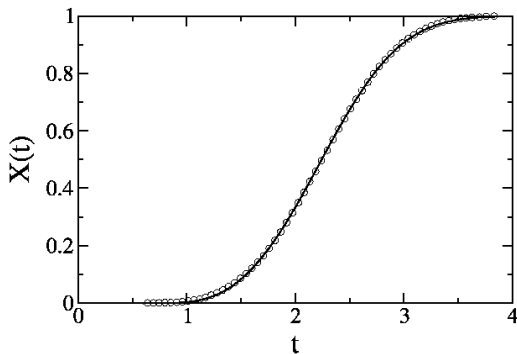


FIG. 1. Transformed fraction $X(t)$ vs time for a 500×500 system. (\circ) numerical integration of Eq. (4) with $W = 1$, $\tau = 0.15$, $\lambda = 0.6$, $\Delta x = 1$, $\Delta t = 0.01$, and $k_B T = 0.1$, averaged over 100 runs. Solid line, KJMA fit with $\tau_i = 0.75 \pm 0.01$ and $\tau_c = 1.68 \pm 0.01$.

Once we have established the connection between the physical system and the model, let us numerically check its capability to reproduce the KJMA equation (2). In Fig. 1 we show the results from simulation using the Euler integration scheme [35], and the corresponding KJMA fit to the fraction of transformed material, $X(t)$, taking $m = 3$ (measured as the fraction of sites where $\phi > 0$). We have reproduced this result for a wide range of parameters. The first important result concluded from these simulations is related to the nonzero value of the incubation time τ_i . This time is almost always present in the experiments, and is related to the free-energy difference between the well $\phi = -1$ and the maximum

of the free-energy separating this well with the one at $\phi = +1$. Similar results were obtained by Elder *et al.* [36] in the context of eutectic growth. Despite the good agreement between simulations and theory, it is important to stress that the derivation of KJMA equation makes use of some assumptions: infinite system size, uniform nucleation, spherical particles, and constant growth rate. Some care must be taken in this respect. Despite Eq. (4) provides circular grains, those grains do not grow at constant velocity. Actually, the grain radius is related to time through the following equation:

$$t = \frac{1}{V} \left[R - R_0 + R^* \ln \left(\frac{R - R^*}{R_0 - R^*} \right) \right], \quad (12)$$

where R_0 is the initial grain radius and V is the grain growth velocity which, in the thin interface limit, is given by

$$V = \frac{3W\lambda\delta g}{\sqrt{8}\tau}. \quad (13)$$

Thus the velocity is constant just after a short time of order R^*/V . Hence there are slight deviations of the numerical data from the KJMA equation up to times of order R^*/V . Besides this, the infinite size condition has not to be fulfilled necessarily. Actually, the KJMA equation is still valid when the number of grains contributing to growth is large, when the system size L , is much larger than the characteristic length scale related to nucleation and growth, $l = (V/N)^{1/3}$, N being the nucleation rate [13]. Finally, the KJMA equation does not take into account interfacial effects that govern the growth just before the grains meet each other, so there are also some differences between the numerical data and the KJMA equation predictions, in this case, at the later stages of the transformation. Fortunately, the mentioned deviations from the KJMA equation at short and long times are quite small. Notwithstanding, it is quite convenient to perform the fitting of $X(t)$ between the 1% and the 99% to improve it (see Ref. [13] for further details about the validity of KJMA equation).

To point out the crucial role played by thermal noise in Eq. (4), we show in Fig. 2 the spontaneous and continuous nucleation and growth of grains, which are almost circular despite the underlying integration lattice is square. In other words, the model captures all the essential ingredients of a first-order transition, not only in terms of the free-energy difference between phases, but also in terms of the dynamical path followed from the metastable phase to the stable one.

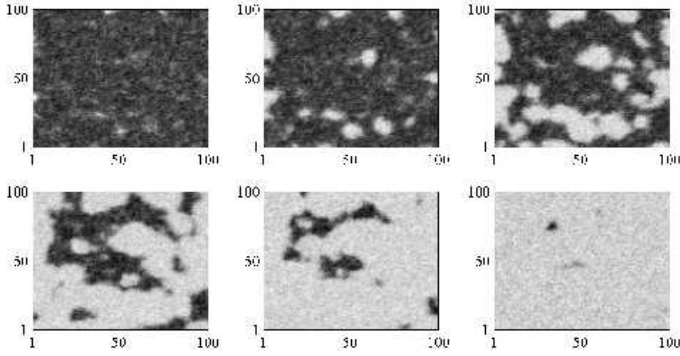


FIG. 2. Numerical integration of Eq. (4) with $W = 1$, $\tau = 0.15$, $\lambda = 0.6$, $\Delta x = 1$, $\Delta t = 0.01$, and $k_B T = 0.1$. From left to right, from top to bottom, corresponding times 1.0, 1.5, 2.0, 2.5, 3.0, and 3.5. The darker sites stand for $\phi \simeq -1$ and the brighter ones for $\phi \simeq +1$. It can be clearly seen how the initial metastable phase evolves into almost circular grains which nucleate and coalesce continuously.

III. NUCLEATION AT DEFECTS

In the previous section we have demonstrated the validity of our model to describe homogeneous nucleation. This section deals with nucleation in the neighborhood of some parts of the system which are structurally different, namely, at domain walls or at the surrounding of foreign particles. Thus we will consider two kinds of defects: Walls and circular defects. Our main assumption here is that the particles in the metastable phase do not interact with the defects, which is included in the model through the boundary condition

$$\frac{\partial \phi}{\partial n} = \nabla \phi \cdot \mathbf{n}|_b = 0, \quad (14)$$

where the subscript b stand for boundary; and n is the normal coordinate to the defect boundary.

In order to clarify the relevance of this boundary condition on nucleation we have integrated Eq. (4) with the prescribed condition (14). Figure 3 shows how nucleation is

enhanced at the walls. Actually, this is the most relevant mechanism of nucleation when the chemical potential difference between phases, $\Delta\mu \propto \lambda$, is small. The situation changes dramatically if we increase λ (or if we raise the temperature). This can be better understood in the context of island formation in which λ can be understood as the flux of particles arriving at the surface. In such case, when the flux of particles is large, islands nucleate everywhere in the sample due to the large probability of dimer formation [3], as can be seen in Fig. 3.

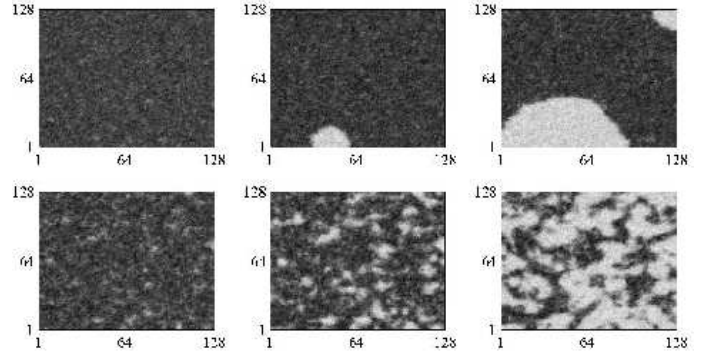


FIG. 3. Numerical integration of Eq. (4) using boundary condition (14), with $W = 1$, $\tau = 0.1$, $\Delta x = 1$, $\Delta t = 0.005$, and $k_B T = 0.15$. The top three figures correspond to $\lambda = 0.35$ at times 1, 5, and 10. The bottom three figures correspond to $\lambda = 0.6$ at times 0.50, 0.75, and 1.00.

As we have mentioned, the other interesting geometry is circular one. Thus Fig. 4 shows how nucleation is enhanced at the boundary of a circular impurity. Moreover, we can use this result to relate the KJMA exponent, m , and the effect of impurities using a finite concentration c , of circular impurities of small radius. The results are plotted in Fig. 5, where time has been rescaled to reveal the differences between several m values, for different temperatures. At this point, we want to stress that this dependence of m on temperature has been obtained qualitatively in some $\text{Pd}_{1-x}\text{Si}_x$ crystallization experiments [38]. Furthermore, if we change the concentration of impurities, we can also modify the value of m (see inset in Fig. 5). This result agrees with that in Ref. [10]. Thus the effect of temperature in KJMA equation is not only present in the characteristic times, τ_i and τ_c , but even in the exponent m in a nontrivial way.

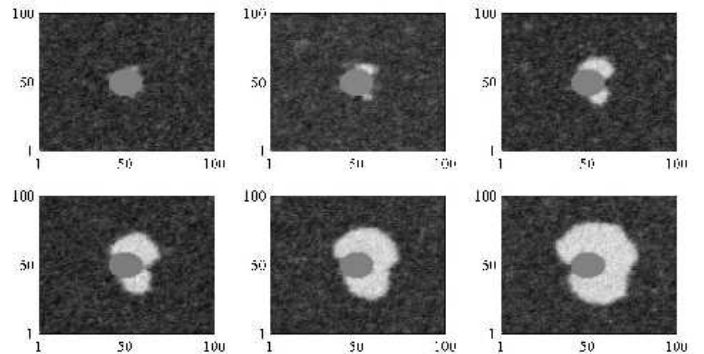


FIG. 4. Numerical integration of Eq. (4) using boundary condition (14) over the circle perimeter, with $W = 1$, $\tau = 0.1$, $\lambda = 0.5$, $\Delta x = 1$, $\Delta t = 0.005$, and $k_B T = 0.1$. From left to right and from top to bottom, corresponding to equally spaced times from 1 to 6.

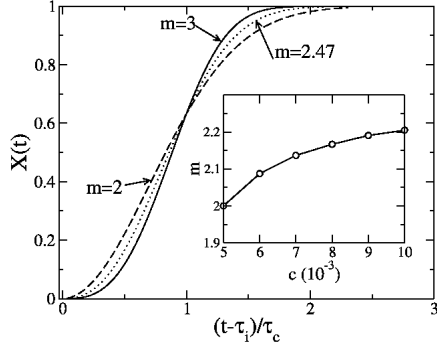


FIG. 5. Fraction of transformed phase $X(t)$ vs scaled time for a 500×500 system, with $W = 1$, $\tau = 0.25$, $\lambda = 0.8$, $\Delta x = 1$, $\Delta t = 0.005$, averaged over 100 ensemble averages using a concentration of impurities $c = 0.005$, and $k_B T = 0.01$ (dashed line), $k_B T = 0.027$ (dotted line), and $k_B T = 0.05$ (solid line). Inset: KJMA exponent m for different values of the concentration of impurities c , with $W = 1$, $\tau = 0.25$, $\lambda = 0.8$, $\Delta x = 1$, $\Delta t = 0.005$, and $k_B T = 0.01$.

IV. GENERALIZED HETEROGENEOUS NUCLEATION

The results reported in the last section demonstrates that our phase field model is a powerful tool to further advance in the knowledge and modeling of nucleation and growth phenomena, in the homogeneous case and in the situation where impurities catalyze the transformation in a subtle way. Notwithstanding, the heterogeneities of a sample are not always due to isolated impurities. This is the main reason for the generalization that we introduce in this section.

We will assume that nucleation is heterogeneous, not in a phenomenological way as in other proposed models [39], but sticking to the classic ideas due to Cahn [40]. Thus the system contains regions with some extra energy (for instance due to some order produced during deposition of the amorphous material), or at which nucleation is more probable. Let us show how we can cast this model on a mathematical footing.

A. Quenched white noise

An intuitive way to introduce the latter idea in our model is sustained on the assumption that the chemical potential depends locally on position,

$$\lambda \rightarrow \lambda + \rho(\mathbf{r}), \quad (15)$$

$\rho(\mathbf{r})$ being a Gaussian random variable with zero mean and correlations given by

$$\langle \rho(\mathbf{r}) \rho(\mathbf{r}') \rangle = \Lambda \delta(\mathbf{r} - \mathbf{r}'), \quad (16)$$

where Λ measures the degree of heterogeneity of the sample. The main part of this generalization is that it does not make any specific assumption about the physical system under consideration. Unfortunately, numerical simulations suggest that it cannot provide a KJMA exponent m , different from 3 (homogeneous nucleation) [37]. Nevertheless, before exploring new possibilities, we will show that the quenched white noise given by Eq. (16) unveils that disorder enhances nucleation (Fig. 6).

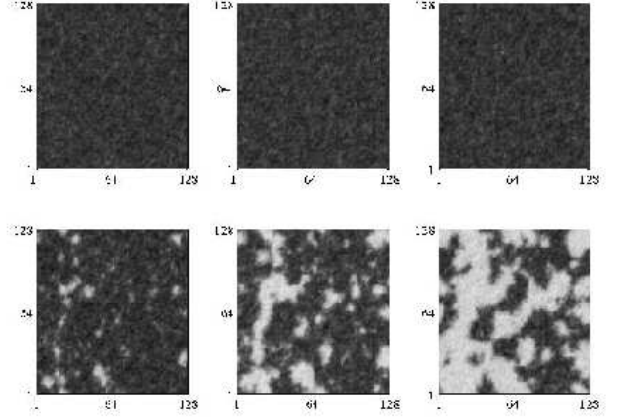


FIG. 6. Comparison between homogeneous nucleation ($\Lambda = 0$, top panels) and heterogeneous nucleation with quenched white noise ($\Lambda = 0.3$, bottom panels), at different times (from left to right: $t = 20, 50$, and 100) with: $W = 1$, $\tau = 1$, $dx = 1$, $dt = 0.005$, $k_B T = 0.1$, and $\lambda = 0.4$.

The fact that white noise is not capable to provide realistic values of m stems with intuition but, actually, it is very physical. Let us make some calculations to show it clearly. If we perform again the thin interface limit of Eq. (4) with $\lambda \rightarrow \lambda + \rho(\mathbf{r})$, we obtain the stochastic version of Eq. (9). Hence:

$$\Delta \mathcal{F} = 2\pi R \sigma_l - \pi R^2 \Delta \mu / \Omega + \chi(R), \quad (17)$$

where $\chi(R)$ is given by

$$\chi(R) = \delta g \int d\mathbf{r} \rho(\mathbf{r}) \Theta(r - R), \quad (18)$$

Θ being the Heaviside step function. The new noise term $\chi(R)$ has also zero mean and correlations given by:

$$\langle \chi(R) \chi(R') \rangle = \delta g \Lambda \pi R^2 \delta(R - R'). \quad (19)$$

For brevity, we denote $F = \Delta \mathcal{F}$, $F_0 = 2\pi R \sigma_l - \pi R^2 \Delta \mu / \Omega$ and $D(R) = \delta g \Lambda \pi R^2$. Consequently, for every value of R the free energy is a random number with a distribution given by (recall that ρ is Gaussian)

$$P(F) = \frac{1}{\sqrt{2\pi D(R)}} e^{-(F-F_0)^2/2D(R)}. \quad (20)$$

Taking into account that $\exp[-\Delta\mathcal{F}(R)/k_B T]$ can be understood as the barrier that has to be overcome to create a nucleus of radius R , the critical radius will be simply the one which minimizes that barrier. In the simplest case where $\Lambda = 0$, this minimum is the same as the maximum of $\Delta\mathcal{F}$, but the situation changes because now $\Delta\mathcal{F}$ is a random variable. Thus in the physical system, we can only obtain information about its mean value:

$$\langle e^{-F/k_B T} \rangle = \int dF e^{-F/k_B T} P(F) = \exp \left[\frac{D(R)}{2(k_B T)^2} - \frac{F_0}{k_B T} \right] \quad (21)$$

To be more specific, the critical radius is the solution of

$$\frac{d}{dR} \left(\frac{D(R)}{2k_B T} - F_0 \right)_{R=R^*} = 0 \Rightarrow R^* = \frac{2\sqrt{2}W}{3\delta g(\lambda + \Lambda/2k_B T)}. \quad (22)$$

This is the result we were seeking: The critical radius diminishes so that the nucleation rate increases and also depends on temperature. But, as we anticipated above, the only effect of quenched white noise is changing the time and length scales of the system, but not the nucleation conditions necessary to obtain $m < 3$. Moreover, if we re-scale both length and time, then the systems with $\Lambda = 0$ or $\Lambda \neq 0$ cannot be distinguished. There is another interesting point of this theory which should be remarked. In some experiments of recrystallization the *a priori* value of $\Delta\mathcal{F}^*$ is actually much smaller than that measured from the experiments [2], confirming that there is some kind of disorder which affects significantly this magnitude.

B. Quenched colored noise

At this point, we must collect some of the successful ingredients of the theory and try to find out which must be the new ones in order to provide a general model of heterogeneous nucleation. Then, the main question is: What was implicit in the approach to heterogeneous nucleation in Sec. III which is missing in Sec. IV A? The answer is related to the new length scale introduced in Sec. III through the concentration of impurities (and which is proportional to $c^{-1/2}$). Therefore we need both ingredients: disorder and a new independent length scale. The simplest way to include both is by means of a quenched colored noise term:

$$\langle \rho(\mathbf{r})\rho(\mathbf{r}') \rangle = \Lambda e^{-(\mathbf{r}-\mathbf{r}')^2/2l_c^2}. \quad (23)$$

For the sake of completeness we have performed the simulations below using Ornstein-Uhlenbeck correlations [35] instead of Gaussian as in Eq. (23), but the results did not change significantly. With this choice we have the same free-energy distribution of probability $P(F)$ as in

the white noise case, and also introduced the required length scale. As we expected, the KJMA exponent m depends on the correlation length l_c as we show in Fig. 7 as also the nucleation rate is larger than in the homogeneous case. These results can be straightforwardly understood in terms of the involved characteristic length scales, the nucleation and growth length scale, $l = (V/N)^{1/3}$, and the quenched noise correlation length, l_c . Thus if $l_c \ll l$ then the system hardly see the defects, and it is almost homogeneous, so $m \simeq 3$. On the contrary, if $l_c \gg l$, as grains nucleate preferentially at the defects, and they grow so fast that they impinge to each other at a mean distance l_c , so there is not enough time to allow other grains to nucleate. Consequently, $m \simeq 2$ because every grain that nucleates does it mainly at the beginning of the transformation. Note that these assumptions are valid whenever both l and l_c are much smaller than the system size L . Notwithstanding, some care must be taken when simulating the model using large values of l_c because the nucleation events are restricted to the surroundings of the defects so there are not many grains to sustain the validity of the KJMA equation.

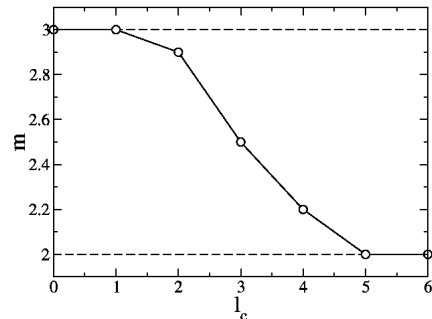


FIG. 7. KJMA exponent, m , for different values of the correlation length, using $W = 1$, $\tau = 0.15$, $\lambda = 0.5$, $\Delta x = 1$, $\Delta t = 0.05$, $k_B T = 0.05$ and $\Lambda = 0.05$. (o) and solid line, results from simulations. The dashed lines are a guide to the eye.

Therefore the latter result contains relevant physical information relative to the basic conditions yielding an exponent $m < 3$. For instance, it is consistent with those crystallization experiments of $\text{Si}_{1-x}\text{Ge}_x$ by Olivares *et al.* [8] or recrystallization of $\text{Pd}_{1-x}\text{Si}_x$ by Price [38]. In the first case that correlation length could be related to the concentration of preexisting SiGe crystals created during deposition, and in the second case with the former polycrystalline structure which has been deformed before recrystallization.

V. DISCUSSION AND CONCLUSIONS

In this paper we investigated a phase field model modeling nucleation and growth events, such as crystallization, island formation, or recrystallization. Starting from a Langevin equation we have shown how it is a simple (and computationally efficient) way to explore homogeneous nucleation, in terms of the well-known description provided by the KJMA equation, Eq. (2). Taking this equation as a starting point, we have provided several approaches to the problem of heterogeneous nucleation. The first approach is related to the existence of defects which are inert for the main growing material, such as wall domains or impurities. In both cases we have shown how nucleation is enhanced near those defects. Moreover, a finite concentration of isolated defects is able to modify the value of the KJMA exponent m , which takes values lower than $m = 3$, the known value for homogeneous nucleation. This kind of defects can be suitable to study secondary crystallization, island nucleation in heteroepitaxial systems (if one of the growing particles presents a slow dynamics compared to the others), or nucleation at step edges in terrace growth. In particular, wall defects can be used to investigate the influence of a terrace step on island formation (note that λ plays the role of the flux of particles arriving at the terrace). In fact, the competition between dimer formation and nucleation at step edges has been reported in Ref. [3], and can be graphically seen in Fig. 3. Generalizing the model to higher dimensions, this kind of wall defect could simulate the glass substrate on which the amorphous material is grown prior to crystallization. In the context of amorphous crystallization, circular defects can also be understood as crystals created at the growing stage, before crystallization takes place.

We have also presented a generalized model for heterogeneous nucleation which deals statistically with imperfections or impurities by means of a quenched noise term. The main result is related to the fact that this quenched noise must be spatially correlated to provide a general description in terms of the KJMA exponent. As we mentioned above, the correlation length can be related to preexisting crystalline regions embedded in the amorphous host or, some deformed polycrystalline structure, but it may also be used to quantify the effect on island formation of mechanical stresses caused by the growth of multilayer devices.

Due to the general character of the model, it can be easily generalized. For instance, a model that takes into account the possible time dependence of the disorder should include two fields: the phase-field and another one related to the motion of impurities. Besides this, sometimes the nucleating grains present some kind of anisotropy that should be included in the free-energy functional, given by Eq. (3). Moreover, the model presented is only suitable for isothermal transformations so, to study non isothermal effects, we should couple the

phase field with an evolution equation for the temperature, similar to some prescriptions provided in the context of non-isothermal eutectic crystallization [41]. Finally, there is some work left to do related to the suitable range of parameters which allow comparisons with experimental data and also to improve the efficiency of the numerical simulations, in particular when using circular impurities to simulate heterogeneous nucleation.

ACKNOWLEDGMENTS

The author thanks A. Sánchez, R. González Cinca, and T. Arribas for useful discussions and helpful comments, and F. Domínguez-Adame for a critical reading of this manuscript. This work has been partially supported by DGES (Spain) Grant No. BFM2000-0006.

* Email address: marioc@upco.es

- [1] J. D. Gunton, *J. Stat. Phys.* **95**, 903 (1999).
- [2] R. D. Doherty, *Prog. Mater. Sci.* **42**, 39 (1997).
- [3] C. Castellano and P. Politi, *Phys. Rev. Lett.* **87**, 056102 (2001), and references therein.
- [4] R. Bergmann, G. Oswald, M. Albrecht, and J. H. Werner, *Solid State Phenom.* **51-52**, 515 (1996).
- [5] J. S. Im and R. S. Sposili, *MRS bull.* **21**, 39 (1996).
- [6] Y. Uemoto, E. Fujii, A. Nakamura, K. Senda, and H. Takagi, *IEEE Trans. Electron Devices* **ED-39**, 2359 (1992).
- [7] Hereafter we will refer to impurity as a *mesoscopic* inert object for the growing material, to be understood as strange particle or imperfection.
- [8] J. Olivares, A. Rodríguez, J. Sangrador, T. Rodríguez, C. Ballesteros, and A. Kling, *Thin Solid Films* **337**, 51 (1999).
- [9] M. Castro, A. Sánchez, F. Domínguez-Adame, and T. Rodríguez, *Appl. Phys. Lett.* **75**, 2207 (1999).
- [10] M. Castro, A. Sánchez, and F. Domínguez-Adame, *Phys. Rev. B* **61**, 6579 (2000).
- [11] M. Grant and J. D. Gunton, *Phys. Rev. B* **32**, 7299 (1985).
- [12] A. Roy, J. M. Rickman, J. D. Gunton, and K. R. Elder, *Phys. Rev. E* **57**, 2610 (1998).
- [13] R. A. Ramos, P. A. Rikvold, and M. A. Novotny, *Phys. Rev. B* **59**, 9053 (1999).
- [14] H.-J. Jou and M. T. Lusk, *Phys. Rev. B* **55**, 8114 (1997).
- [15] A. E. Kolmogorov, *Bull. Acad. Nauk. USSR., Mat. Ser.* **1**, 355 (1937); W. A. Johnson and R. F. Mehl, *Trans. AIME* **135**, 416 (1939); M. Avrami, *J. Chem. Phys.* **7**, 103 (1939).
- [16] V. G. Karpov, *Phys. Rev. B* **50**, 9124 (1994); V. G. Karpov and D. W. Oxtoby, *ibid.* **54**, 9734 (1996).
- [17] X. Y. Liu, *J. Chem. Phys.* **112**, 9949 (2000).
- [18] Y. Enomoto, *Acta Metall. Mater.* **38**, 173 (1990).

- [19] M. C. Weinberg, *J. Non-Cryst. Solids* **225**, 1 (1999).
- [20] R. Kobayashi, *Physica D* **63**, 410 (1993).
- [21] A. A. Wheeler, B. T. Murray, and R. J. Schafer, *Physica D* **66**, 243 (1993).
- [22] A. Karma and W.-J. Rappel, *Phys. Rev. E* **57**, 4323 (1998).
- [23] R. Folch, J. Casademunt, A. Hernández-Machado, and L. Ramírez-Piscina, *Phys. Rev. E* **60**, 1724 (1999); **60**, 1734 (1999).
- [24] K. R. Elder, M. Grant, N. Provatas, and J. M. Kosterlitz, *Phys. Rev. E* **64**, 021604 (2001).
- [25] J. B. Collins and H. Levine, *Phys. Rev. B* **31**, 6119 (1985).
- [26] M. Dubé, M. Rost, K. R. Elder, M. Alava, S. Majaniemi, and T. Ala-Nissila, *Eur. Phys. J. B* **15**, 701 (2000).
- [27] I. Steinbach, F. Pezolla, B. Nestler, J. Rezende, M. Seesselberg, and G. J. Schmitz, *Physica D* **94**, 135 (1996).
- [28] B. Nestler and A. A. Wheeler, *Phys. Rev. E* **57**, 2602 (1998).
- [29] R. Kobayashi, J. A. Warren, and W. C. Carter, *Physica D* **140**, 141 (2000); *J. Cryst. Growth* **211**, 18 (2000).
- [30] A. E. Lobkovsky and J. A. Warren, *Phys. Rev. E* **63**, 051605 (2001).
- [31] The level curve $\phi = 0$ is generally accepted to define the boundary position. Notwithstanding, this is not necessary and, in order to obtain the correct sharp-interface limit of some phase-field models, other values can be more suitable (see Ref. [24] for further details).
- [32] P. C. Hohenberg and B. I. Halperin, *Rev. Mod. Phys.* **49**, 435 (1977).
- [33] For completeness we have reproduced the numerical simulations presented in Secs. III and IV using $g(\phi) = \phi - 2\phi^3/3 + \phi^5/5$, but the results were not affected by the specific choice of g .
- [34] R. Becker and W. Döring, *Ann. Phys. (Leipzig)* **24**, 719 (1935); Ya. B. Zeldovich, *Acta Physicochim. (URSS)* **18**, 1 (1943).
- [35] C. W. Gardiner, *Handbook of Stochastic Methods* (Springer-Verlag, Berlin, Heidelberg, 1985).
- [36] K. R. Elder, F. Drolet, J. M. Kosterlitz, and M. Grant, *Phys. Rev. Lett.* **72**, 677 (1994).
- [37] Similar results were found by M. Karttunen, N. Provatas, T. Ala-Nissila, and M. Gardner, *J. Stat. Phys* **90**, 1401 (1998), in the context of flame fronts in slow combustion.
- [38] C. W. Price, *Acta Metall. Mater.* **38**, 727 (1990), and references therein.
- [39] H. J. Frost and C. V. Thompson, *Acta Metall.* **35**, 529 (1987).
- [40] R. W. Cahn, *J. Inst. Met.* **76**, 121 (1949).
- [41] K. R. Elder, J. D. Gunton, and M. Grant, *Phys. Rev. E* **54**, 6476 (1996).